

Module 4: Interferometry

Lecture 18: Applications, literature review, interferometry

The Lecture Contains:

☰ Introduction

- Applications
- Optical Methods
- Image Processing and Tomography
- Scope of the present work

☰ Review of Literature

- Interferometry
- Holographic Interferometry
- Computerized Tomography
- Interferometric Tomography
- Crystal Growth
- Other Techniques
- Text Organization

☰ Laser Interferometry

- Laser Source
- CCD Camera
- Pneumatic Isolation Mount
- Alignment of the Interferometer
- Recording Interferometric Projections

◀◀ Previous Next ▶▶

Module 4: Interferometry

Lecture 18: Applications, literature review, interferometry

Introduction

Nonintrusive techniques are being extensively used in engineering measurements. These techniques employ radiation sources as probes. All radiation-based measurements share a common feature in that they generate images of a cross-section of the physical domain. This is to be contrasted with mechanical probes which are concerned with measurements at a point in space and can accomplish this task only after the field to be studied has been physically perturbed. Radiation methods are also inertia-free. Hence, the scanning of a cross-section of the physical region using radiation-based probes results in a large volume of information with practically no time delay.

Applications

Laser-based optical techniques have reached a high degree of maturity. Optical methods such as laser Doppler velocimetry have replaced traditional methods such as pilot tubes and hot-wire anemometry. Flow visualization methods of the past have evolved to a point where it is now possible to gain qualitative understanding of the flow and transport phenomena. Sophisticated measurement techniques such as Rayleigh and Mie scattering for temperature and concentration measurement and Raman spectroscopy for detection of chemical species in reacting flows are routinely employed in engineering research. Using satellite radar interferometry, orbiting instruments hundreds of kilometers away in space, can detect subtle buckling of the earth's crust and thus detect minerals and oil predict volcanic eruptions. Integrating techniques of photography and video recording, digital image processing, optics and color measurement, it is now possible to map the fluid surface slopes of oceans, rivers and lakes optically into color space. Using reconstruction techniques, the surface elevations can then be back-calculated. If the fluid surface is relatively flat, the spectrum of the reflected light contains rich information about the temperature variation over it. Radiation-based measurements from the backbone of satellite instrumentation, weather prediction programs and defence weaponry.

Buoyancy-driven convection is encountered in a large number of engineering applications such as cooling of electronic equipment, solar ponds, stratified fluid layers in water bodies, and materials processing to name a few. Studying convection patterns is also of importance in nuclear power plants. Specific examples include passive heat removal in advanced reactor systems, stratification phenomena in steam vessels in which hot and cold water streams mix, and thermal pollution in reservoirs. The liquid metal pools in fast breeder reactors is also subjected to stratification.

Measurements of the shape of the fluid surface and temperature distribution over it are critical for studies of near surface dynamics. There has long been interest in understanding the behavior of short surface wind waves because of their importance in mass, momentum, and energy exchanges at the air-sea interface, in microwave remote sensing of the sea surface, and in the theory of wave-wave interactions. Associated problems of great interests are (a) the interaction of a free vortex with a free surface, (b) behavior of turbulence near the free surface, and (c) the effect of a variable surface tension on the shape of the free surface. A free vortex approaching the free surface may deform the surface and cause the vortex line to be connected to it. Thus, bursts originating from the lower heated wall can modify the air-water interface and significantly alter the local transport rates.

A special application where laser optics can be profitably used is in the growth of a crystal from its supersaturated aqueous solution. Crystals with a high degree of perfection are required for important and sensitive high-technology applications. **Examples are the semiconductor industry** for making computer chips and optically transparent materials for making high-power lasers. Growing methods for

high-quality crystals include melt growth, flux growth and solution growth. Each of the crystal-growing processes is determined by principles of physico-chemical hydrodynamics and is extraordinarily complex. To control the process and ensure growth of large high quality crystals, it is important to understand the physical phenomena involved during crystal growth. These include all modes of heat transfer, phase change, interfacial transport, and turbulence in complex geometries. Hence, there is a need to understand the thermofluid mechanics of the crystal growth mechanism.

Measurements of the temperature and concentration fields around a crystal growing from an aqueous solution, the surface morphology, and the kinetics of major faces of the crystal is a critical engineering application. The crystal is grown in a specially-designed growth cell under controlled temperature conditions. Under growing conditions, spatio-temporal fields of temperature and concentration are setup around the crystal. The growth mechanism of the crystal, as well as its morphology, are intricately linked to temperature and concentration gradients at the crystal surface. Since these gradients setup a density field as well, the crystal will experience buoyancy-driven fluid motion around it. The solution around the crystal can be optically mapped to generate the full three-dimensional information of the scalar fields. They can be controlled **online** with the objective of enhancing the **insitu** quality of the growing crystal.

 **Previous** **Next** 

Optical Methods

When the wavelength of the radiation used is in the visible range, the measurement procedure classifies as an **optical technique** and the region being scanned appears on a screen as an image that is visible to the naked eye. In thermal sciences, a revival of optical techniques for temperature and velocity measurements in fluids has occurred. Possible reasons for this developments are:

- Commercially available lasers have a high degree of coherence (both spatial and temporal) and are cost-effective.
- Optical images can be recorded conveniently through computers and can be processed as a string of numbers through numerical algorithms.

The implications are that coherence generates stable image patterns, which truly reflect the flow behavior, and computer programs now simplify and replace very tiring microscope operations. The image formation can be related to the patterns formed by solid particles suspended in the fluid, attenuation of radiation, scattering or the dependence of reflectivity and refractive index on temperature. Optical methods that utilize the dependence of *refractive index* of light on quantities such as density, concentration and temperature can be configured in many different ways. Three available routes are:

1. Shadowgraph, where the reduction in light intensity on beam divergence is employed,
2. Schlieren, where light deflection in a variable refractive-index field is captured, and
3. Interferometry, where the image formation is related to changes in the refractive index with respect to a reference environment.

For a wide class of applications where temperature differences are within certain bounds, interferometry appears to be a versatile tool for accurate measurement of three-dimensional unsteady temperature field, and with some modification, for velocity fields. Many examples involving free, mixed, and forced convective heat transfer are included in this category. Worth mentioning is the satellite-based imaging of the planetary atmosphere using coherent optics. In this context, issues such as evaluation of model constants in weather prediction codes, and stabilizing these codes using images of the flow field are being addressed.

The author's experience is with a Mach-Zehnder interferometer for studying two- and three-dimensional temperature fields in buoyancy-driven flows with air as the working fluid. Steady as well as slowly evolving fields have been considered. Flow configurations that have been addressed are:

The Mach-Zehnder interferometer for studying two- and three-dimensional temperature fields in buoyancy-driven flows with air as the working fluid. Steady as well as slowly evolving fields have

been considered. Flow configurations that have been addressed are :

1. Natural convection from a discrete protruding heater mounted on a vertical wall.
2. Rayleigh-Benard convection in a two-dimensional square cavity.
3. Tomographic reconstruction of three-dimensional temperature field using interferograms.
4. Rayleigh-Benard convection in a horizontal fluid layer at high rayleigh numbers.
5. Buoyancy-driven convection in axisymmetric geometries.

The Mach-Zehnder interferometer used in the present work employs a **35mW** He-Ne laser and **150mm** (diameter) optics. Interferograms are recorded using a CCD camera with a **512 × 512** pixel resolution. The camera is interfaced with a PC through an 8-A/D card which digitize light intensity levels over a range of 0 to 255. Image acquisition is at video rates (**50frames/s.**)

◀ Previous Next ▶

Image Processing and Tomography

The fringe patterns produced by the interferometer need to be converted into records of the fluid temperature. This step requires identifying intensity minima within fringes (*fringe thinning*), locating fringe edges (*edge detection*), determining fringe order, and measuring distances between fringes. Since the image is recorded through a computer, these operations can be performed with computer programs. In most real life experiments, this step is difficult since operations such as locating fringe minima and edges result in ambiguity. One of the factors that causes difficulties in identification is speckle, a form of noise. Elaborate procedures must then be employed to remove speckle from the interferometric images. Examples of cleaning strategies are Fourier-filtering using band-pass filters, histogram specification, and Laplacian smoothing.

Let $n(x)$ and $T(x)$ be the refractive index and temperature fields, respectively, in the physical domain being studied. Let n_0 and T_0 be their reference values, as encountered by the reference beam. The interferogram is a fringe pattern arising from the optical path difference

$$\Delta PL = \int (n - n_0) ds \quad (1)$$

which in terms of temperature is

$$\Delta PL = \frac{dn}{dT} \int (T - T_0) ds \quad (2)$$

The integral is evaluated along the path of a light ray. Neglecting refraction effects, this path will be a straight line and the integral evaluation is greatly simplified. As a special case, if the flow field is two dimensional (*say in the $x - y$ plane*), then the light beam can be oriented in the z -direction and the equation above reduces to

$$\Delta PL = \frac{dn}{dT} (T - T_0)L \quad (3)$$

where L is the length of the test cell parallel to the direction of the light beam.

In a more general setting, when the temperature field is three-dimensional, recovering $T(x)$ from a single image is not possible. This image can, however, be viewed as a projection of the temperature field in the s -direction. If the original field is three-dimensional, its projection is a field in a dimension reduced by unity, i.e., two for the present case. It is theoretically possible to record a very large number of projections of the test fields in many directions, and in the practical problems, it is not possible to record too many projections, either due to limitations of the experimental setup or due to cost. This process of three-dimensional reconstruction from two-dimensional projections is called **tomography**.

In practical problems, it is not possible to record too many projections, either due to limitations of the experimental setup or due to cost. A new subject has now evolved which is concerned with reconstruction with only a few views and is called limited-view tomography. Some of the popular methods used here are algebraic reconstruction techniques (ART), multiplicative algebraic reconstruction technique (MART), and maximum entropy (MENT). These techniques are iterative in nature and reconstruct the unknown function over a grid.

Scope of the present work

Laser interferometry is a powerful measurement technique to record temperature fields in a fluid medium. Combined with tomographic algorithms, the method can reconstruct three-dimensional temperature fields. The review covers interferometric measurements, image processing operations for enhancement of interferograms, evaluation of fringe patterns, and limited-view tomographic algorithms. Experimental results for a variety of buoyancy-driven flow problems have also been presented. The paper is organized under the following sections: Review of literature, laser interferometry, Image processing, Data reduction, Computerized tomography, and Applications.

 **Previous** **Next** 

Review of Literature

Interferometry

Optical methods have been employed sporadically for heat transfer measurements over the past 50 years. The convenience of lasers as light sources and computers for data acquisition and processing has resulted in a resurgence of this technique in the past decade. Recent developments have been summarized in a special issue of *Optics & Laser Technology* (February, 1999) on "Optical Methods and Data Processing in Heat and Fluid Flow". In more general setting, new and novel measurement technologies can be seen in the proceedings of the biennially held International Symposium on Flow Visualization and the Pacific Symposium on Flow Visualization and Image Processing. A survey of interferometry as applied to natural convection problems is presented below.

An early review of optical methods in heat transfer has been presented by Hauf and Grigull [1]. Chu and Goldstein [2] have reported a study of turbulent convection in a horizontal layer of water for the classical Rayleigh-Benard problem. Mach-Zehnder interferometer was employed by the workers for flow visualization. Lewis et al [3]. have investigated the development of mixing-layers in laboratory experiments concerning salt-stratified solutions that are initially stable, but are destabilized by a temperature difference in the vertical direction. Goldstein [4] has surveyed optical technologies for flow and temperature measurement. Lauterborn and Vogel [5] have reviewed the status of optical techniques in fluid mechanics. Mayinger [6, 7] has reviewed image forming optical techniques in heat transfer and computer-aided data processing. Tolpadi and Kuehn [8] have reported a computational and experimental study of a three-dimensional temperature field in an asymmetric geometry. The heat transfer problem involves conjugate conduction-convection and the thermal field in both the solid and fluid phases have been visualized using interferometry. These authors have compared the performance of several reconstruction algorithms applied to experimental data against the numerical solution. The Grid method was found to have the greatest accuracy. Naylor and Tarasuk [9] have presented a computational technique for processing interferograms that are seen in buoyancy-driven convection. Muralidhar et al. [10] have studied the transient natural convection in a square cavity in the intermediate Rayleigh number range using a Mach-Zehnder interferometer. Evaluets-Lehnoff et al. [11]. Chandrasekhara et al. [12] have discussed a high-speed phase-locked interferometry system that has been designed and developed for real-time measurements of dynamic stall flow over a pitching aerofoil. Zhong and Squire [13] have used interferometry to evaluate organized structures in high-speed flow past a circular cylinder. They have reported the similarities between compressible and incompressible wakes as well as similarities in the turbulent structures. Dupont et al. [14] have discussed the use of electronic speckle interferometry for visualizing isotherms as well as streamlines in a Rayleigh-Benard configuration. Dietz and Balkowski [15] have discussed the estimation of refraction errors in two-dimensional supersonic boundary layers. Most recently, Optical methods for flow and heat transfer have been reviewed by Lehner and Mewes [16].

Holographic Interferometry

Mapping of three-dimensional temperature fields can be accomplished using principles of holography. An algorithm for evaluating holographic interferograms has been presented by Aparicio et al. [17]. Applications of holographic interferometry to heat transfer can be seen in the work of Matulka and Collins [18], Shattuck et al. [19], Spatz and Poulidakos [20], and Shen and Poulidakos [21]. Beer [22] has reported interference fringes in growing steam and refrigerant bubbles from a heated surface. Temperature fields within the bubble also have been presented in this work. Faw and Dullforce [23] have investigated convective heat transfer beneath a heated horizontal plate in air using holographic interferometry. The application of tomography to holographic interferometry has been reported by Ostendorf et al. [24]. Bahl and Liburdy [25] have studied three-dimensional temperature reconstruction above a horizontal heated disk in air using holographic interferometry. Computerized holographic measurement in supersonic flow past bluff objects has been discussed by Lanen [26] and Lanen et al. [27]. The author of this article has experienced difficulties with the holographic route, primarily due to unavailability of the plates necessary for recording holograms. This has led to the route of storing interferograms on computers, followed by a tomographic inversion to recover the three-dimensional temperature field.

 **Previous** **Next** 

Computerized Tomography

A considerable amount of literature is presently available in the area of tomographic algorithms. These algorithms work with a set of projections of the field being investigated and reconstruct it to a certain degree of approximation [28]. They can be broadly classified as: (a) Transform methods, (b) Series expansion methods, and (c) optimization techniques. The first leads to the explicit calculation of the reconstructed field via the **Radon Transform**. Practical implementation of this method involves the use of convolution integrals and is called the convolution backprojection (CBP) algorithm. The second and third are iterative in nature and have been developed with a view towards handling a limited number of projections. In interferometry applied to measurement of temperature fields in fluids, the series expansion method is best suited. Censor [29] has reviewed the series expansion methods in terms of their rate of convergence and accuracy. Gull and Newton [30] have discussed the use of maximum entropy principle in tomographic reconstruction. A method of encoding prior information has been discussed. Verhoeven [31] has reported the performance of state-of-the-art implementation of a MART (Multiplicative Algebraic Reconstruction Technique) algorithm to multidimensional interferometric data. Subbarao et al. [32] have compared ART (Algebraic Reconstruction Technique), MART, and entropy-based optimization algorithms for three-dimensional reconstruction of temperature fields. A detailed error analysis has been presented: The principal findings of their study is that MART gives the best all around performance even with as few projections as two.

Interferometric Tomography

Snyder and Hesselink [33] introduced the idea of combining holographic optical elements with tomography, thus permitting high-speed, high-resolution flow visualization. In a similar work aimed at recording microsecond events at a high-speed, Zoltani et al. [34] have used a flash X-ray source. Gmitro and Gindi [35] have described an electrooptical device that can perform reconstruction with the CBP algorithm at video-rates. The idea here is to use optical elements to carry out some of the numerical integration needed for three-dimensional reconstruction. Tomography applied to interferometric data can be seen in the work of Faris and Byer [36] for supersonic jets where refraction effects have been accounted for. Snyder [37] has studied species concentration in a co-flowing jet using tomographic interferometry. Liu et al. [38] used photographs to initiate tomographic reconstruction and have applied the method to axisymmetric and asymmetric helium jets. Watt and Vest [39] studied structures of turbulent helium jets in air by recording the path integral images based on the refractive index variation using a pulsed phase-shifted interferometer. The advantage of this method is that one can record the phase of the light wave as continuous data, rather than discrete fringes. This greatly improves the spatial resolution of the measurement, being the pixel size rather than the fringes spacing. Subsequently, the authors have tomographically reconstructed the helium concentration field. Tomographic measurement techniques and the appropriate reconstruction algorithms suitable for the process industry have been discussed by Mews et al. Michael [40] and Yang [41] have discussed three-dimensional reconstruction of the temperature field using an iterative technique. A Mach-Zehnder interferometer was used in this work on Rayleigh-Benard convection with water as the working fluid. Bahl and Liburdy [42] have discussed tomographic reconstruction for a synthetic temperature field. Soller et al. [43] applied iterative tomographic techniques to study interaction of supersonic jets and independently to buoyancy-driven convective flow around a light bulb. They have noted significant advantages in the tomographic approach, particularly when the recorded data is incomplete. Sato and Kumakura [44] developed the dual plate Fourier transform interferometry to improve the spatial resolution of the measurement by introducing a carrier frequency that modulates the usual fringe patterns. This instrument has then been used to map the thermal field in premixed flames.

Crystal Growth

Optical methods have been employed in crystal growth research for around half a century. The exploitation of lasers as light sources and computers for data acquisition and processing is very recent. Laser-interferometry is evolving as a powerful technique in studying online and *in situ* crystal growth phenomena. This application is of considerable importance because the grown crystals can be used in high-technology applications, i.e., solid-state lasers. The crystal growth technology being referred to here is the growth of crystals from their supersaturated aqueous solutions. Once the growth process is initiated, temperature, and concentration gradients are setup in the liquid phase around the crystal. These in turn can lead to buoyancy-driven currents and influence the crystal quality. The objectives behind measurement are then to monitor the flow, thermal and concentration fields in the solutions, and also the surface topography of the grown crystal. The thermal and concentration fields can be mapped using refractive index-based techniques; it is interesting to note that the crystal surfaces can be mapped using differences in the geometric path length, as in a Michelson interferometer. A brief survey of laser-interferometry applied to research on fluid mechanics and transport phenomena during crystal growth is presented below.

The observation of growth spirals using phase contrast microscopy (PCM) was first reported by Verma [45]. Similar microscopy studies were carried out by Sunagawa [46] on mineral crystals and summarized later by the author [47]. Extensive work on the surface microtopographic investigations of solution grown crystals using PCM and DICM (differential interference contrast microscopy) has been carried out by Bennema and coworkers [48]. They observed the spirals on crystals growing from the liquid state. Tsukamoto et al [49, 50]. demonstrated that by combining optical phase contrast microscopy and differential interference contrast microscopy with a convectional TV system, mono-molecular spiral growth steps on crystals can be observed during the growth in aqueous solution. Onuma et al. [51-53] have carried out a study of crystal growth at the microscopic level on barium nitrate and K-alum using Schlieren and Mach-Zehnder interferometry. They studied the effect of buoyancy driven convection and forced flow rate on the microtopography of the crystal growing from solution. Maiwa et al. [54] studied the growth kinetics of faces of barium nitrate crystals using micro-Michelson interferometry in conjunction with the differential interference contrast microscopy. Onuma et al. [55-56] developed a real-time phase shift interferometer, an improvement over the DICM, and applied it to the measurement of the concentration field through a micro-Mach-Zehnder interferometer. Simultaneously they used a micro-Michelson interferometer to study the growth kinetics. Later Sunagawa [57] reviewed the research carried out by his coworkers on interferometric analysis of crystal grown from the solution.

In addition to the Japanese researchers listed above, the work carried out by Chernov, Rashkovich, and Vekilov and their coworkers in Russia has helped in understanding the mechanics of solution-grown crystals. Rashkovich et al. [58-64] developed a Michelson interferometer for studying the growth rate, slope of growth hillock, step velocity, and the hydrodynamics of the solution around crystals growing from it. Their experimental setup can be used for studying crystals as small as a few millimeters to as large as several centimeters. Vekilov [65-67] applied Michelson interferometry to the study of KDP and ADP crystal growth kinetics, as well as to understand protein crystal growth mechanism. Sherwood and his coworkers at Glasgow have also used interferometry for studying crystal growth rates [68-69]. They have used synchrotron X-radiation for assessment of the strain in crystals and its relation to growth rate dispersion.

Other Techniques

Schlieren and shadowgraph are the other two techniques besides interferometry, that can be used to form images of the thermal field using refractive index changes. The advantages of these methods are a simpler optical configuration, better spatial resolution since the image is an intensity distribution rather than fringes, and suitability for large thermal gradients. The disadvantage arises from the fact that the intensity variation is related to the derivatives of the refractive index field, rather than the refractive index itself. Specifically, a schlieren system can capture the temperature gradient, while a shadowgraph yields the second derivative of the temperature distribution. These distributions can be evaluated in three dimensions, once again by using principles of tomography. The temperature field in principle, can be determined by integrating the gradient field. In practice this can be cumbersome and these two methods continue to be in use primarily for flow visualization. In some problems, the temperature gradient itself may be primary quantity of interest, for example the local Nusselt number on a solid wall. The schlieren image generates a visual picture of the local heat transfer rates, and hence, on occasion can be a superior measurement technique in comparison to interferometry. A review of schlieren and shadowgraph techniques can be seen in the edited books of Goldstein [4] and Mayinger [6].

The application of the schlieren technique to problems of practical importance have been reported by the following authors. Kosugi et al. [70] have experimentally recorded gas temperature profiles in the shock region of excimer lasers and correlated them to the xenon concentration in a helium gas. Koreeda et al. [71] have studied shock structure in air at very high Mach numbers (up to 35) using schlieren signals recorded by a split photodiode. Agrawal et al. [72] have developed a color schlieren technique coupled with tomography for measurement of temperature in gas flows. Bystrov et al. [73] report extraction of the density and temperature fields in shock tube experiments. using schlieren signals.

Coherent structures in a mixing layer were visualized using shadowgraphy by Brown and Roshko [74] in an early pioneering experiment. Images of shocks in high-speed gas flow can be seen in the exhaustive compilation of Van Dyke [75]. Convective flow in a water-filled square cavity with differentially heated side walls has been visualized by a shadowgraph technique by Schopf et al. [76]. The images have been quantitatively evaluated by comparison to a numerical solution of an identical problem.

Schlieren and shadowgraph are popular measurement techniques in the aerospace industry where qualitative yet reliable information is required on shocks, boundary-layers, and their interaction.

Text Organization

In the following sections, principles of laser interferometry, image processing, data analysis, and computerized tomography have been discussed. Interferometric experiments of buoyancy-driven flow have been separately discussed in detail. The discussion in the following sections contains material drawn from Darbhe and Muralidhar [77], Muralidhar et al. [10], Mishra et al. [78], and Mishra et al. [79-82].

Laser Interferometry

The primary instrument used in the present work for temperature measurement in the fluid medium is the Mach-Zender interferometer. Figure 4.9 is a schematic drawing of the interferometer. The optical components present in it, namely the beam splitters BS1 and BS2 and mirrors M1 and M2, are oriented at an angle of 45 degrees with respect to the laser beam direction. The first beam splitters BS1 splits the incoming collimated beam into two equal parts- the transmitted and the reflected beams. The transmitted beam 2 is labeled as the test beam and the reflected beam 1 as the reference beam. The test beam passes through the physical region where the convection process is in progress. It is reflected by the mirror **M1** and recombines with the reference beam on the plane of the second beam splitter (BS2). The reference beam undergoes a reflection at mirror **M2** and passes through the reference medium unaltered and is superimposed with the test beam at BS2. The two beams on superposition at the second beam splitter BS2, produce an interference pattern. This pattern contains the information of the variation of refractive index in the test region. For measurements in air, the reference medium is simply the ambient. For liquids, a compensation chamber is required to introduce an appropriate reference environment. The mirrors and beam splitters employed in the present configuration are of 150 mm diameter. The beam splitter has 50% reflectivity and 50% transmittivity. The mirrors are coated with 99.9% pure silver and employ a silicon dioxide layer as a protective layer against oxidation.

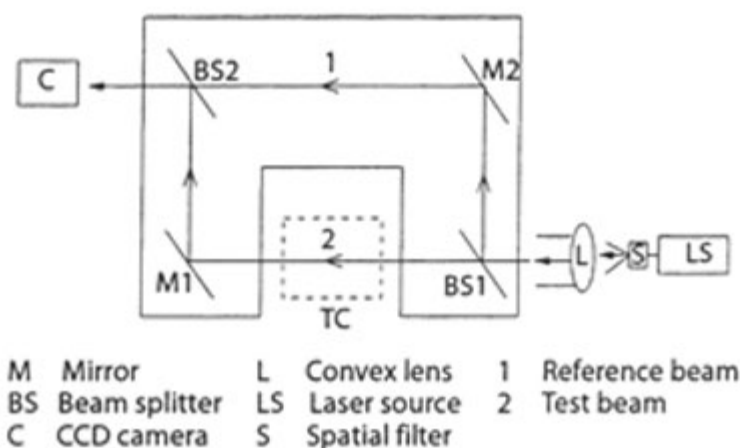


Figure 4.9: Schematic drawing of the Mach-Zender interferometer.

[more...](#)

Laser Source

A 35 mW, continuous wave He-Ne laser ($\lambda = 632.8 \text{ nm}$) is employed as the coherent light source for the interferometer. This laser is sturdy in construction, economical, and stable in operation. The original laser beam is of 2 mm diameter. A spatial filter along with a convex lens or a concave mirror is required to expand the beam to any convenient size. In the present study, the expanded beam diameter is 70 mm. The spatial filter is a lens-pinhole arrangement with two adjustable screws. The distance between the pin hole and have to be adjusted so that the small laser beam is focused on the pin-hole and the outgoing beam is expanded. The specifications of the laser used in the present work are given in [Table 1](#).

CCD Camera

A CCD (charged couple device) camera (Pulnix, model: T5 565) of spatial resolution of 512 X 512 pixels has been used to capture the interferometric images. The fringes formed at the second beam splitter of the Mach-Zehnder interferometer are projected on to a screen. The selection of the screen material and collection of interferometric images from it is an important step. This is because the clarity in the images will reduce the uncertainty in the subsequent calculations. For this purpose, tracing sheet has been used to display the interferometric images in the present work. The attenuation of the laser beam through the thickness of the paper of the paper was found to be small. It was observed that two screens used together with one of them physically perturbed led to distinctly clear images on the video monitor. This effect can be understood as a spatial averaging of the images over the two screens which suppresses noise by superposition and makes the fringe pattern clear.

The CCD camera is connected to a PC-based image processing system through an 8 bit A/D card (Pip 1024 Matrox). The fringe pattern is stored in an integer matrix from with intensities varying between 0 to 255 (the gray scale), where 0 indicates black and 255 indicates white. With the present setup the image acquisition speed is at video rates , namely 50 frames per second. The digital output of the CCD camera is projected to a high-resolution video monitor to visualize, and focus the fringe patterns.

Module 4: Interferometry

Lecture 18: Applications, literature review, interferometry

Pneumatic Isolation Mount

The optical components of the interferometer are extremely sensitive to vibrations. This can be experienced from the movement of the fringes which form on the screen. To avoid ground vibration from reaching the optics, the entire interferometer is placed over four pneumatic isolation mounts. These mounts are connected to an air compressor for pressurization. Once the mounts are pressurized the entire interferometer floats over the mounts. This stabilizes the interferometric images and facilitates image acquisition. An air compressor of rated capacity 10 atmospheres has been used throughout the experiment to pressurize the mounts. The operating pressure for the mounts is 5 kg/cm². A regulator valve was used to supply air to the mounts at the right pressure. The compressor in turn was located sufficiently far away from the interferometer to eliminate motor vibration.

Alignment of the Interferometer

Before the start of the experiment the interferometer has to be aligned. Though the initial alignment of the interferometer is generally not disturbed from one experiment to the other, periodic fine tuning is essential to ensure that the interferometer is operating at its highest sensitivity. The initial alignment of the interferometer is carried out as per the following steps:

1. The light output of the spatial filter is adjusted so that the diffraction rings, which appears with the expanded beam, vanish. This requires adjustment of the screws on the spatial filter. In most experiments, the diffraction ring formed a complete circle and remained outside the periphery of the expanded beam.
2. The laser power output is measured using a light meter. The laser-power output is generally not a stable quantity and changes with time. This change in power output is generally not a stable quantity and changes with time. This change in power output is not a transient phenomena. Instead, it decreases steadily with the hours of operation. During the present work, the laser output was in the range 30-32 mW over two years.
3. The convex lens is adjusted from the pinhole of the spatial filter so that the distance of separation is the focal length of the lens. This produces a parallel laser beam needed for the experiments.
4. All the optical components of the interferometer are adjusted until their centers fall on a horizontal plane. Once this is accomplished, the first beam splitter is adjusted until it is at 45 degrees to the incoming light rays. All the remaining optical components are then made parallel to one another by turning one at a time. The mirrors and beam splitters being of 150 mm in diameter, the expanded beam of 70 mm diameter is made to pass through the central portion of the optical components.
5. Adjustment for the infinite fringe setting is delicate and requires effort. In the infinite fringe setting, the initial field-of-view is one of the complete brightness since interference is constructive. The geometrical and the optical path lengths of the test and reference beams are then the same in the absence of any thermal disturbances in the path of the test beam. Owing to imperfect adjustment of the mirrors and beam splitters by screws moment, the exact infinite fringe setting, the distance between the fringes increases and the number of fringes decreases until the illuminated spot is spanned by one or two broad fringes. In the present work, it was possible to reduce the number of fringes to unity at the start of all the experiments. (Fig 4.10)

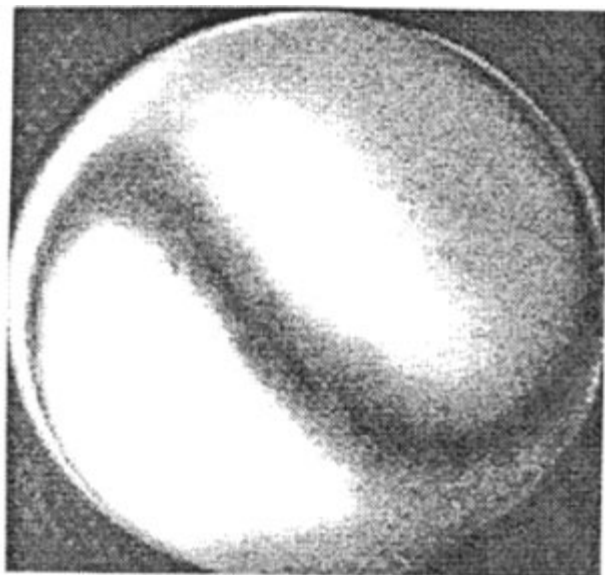


Figure 4.10: Infinite fringe setting of the interferometer

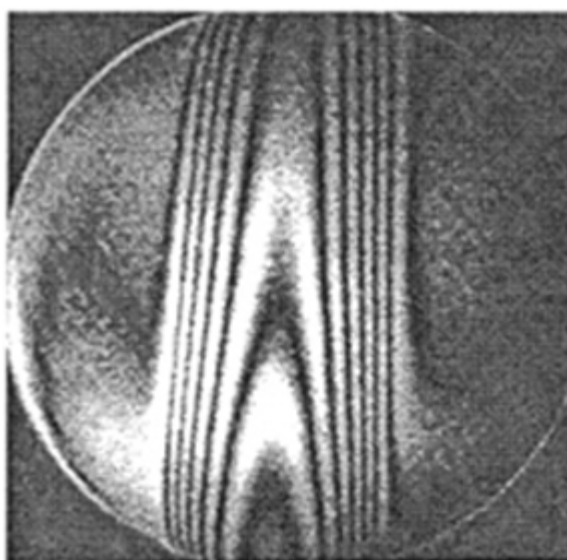


Figure 4.11: Candle Flame in the infinite fringe setting

[more...](#)

[◀ Previous](#) [Next ▶](#)

Recording Interferometric Projections

When the method of axial tomography is employed, projection data of the field to be reconstructed has to be recorded from various angles. The experiments with the differentially heated fluid layer were conducted by turning the convection test cell with reference to the light source. The position of the light source and the detector remained fixed in all the experiments. The experiments were conducted at various angles and for each angle the full width of the fluid layer was scanned. The width of the fluid layer being 500X500 mm in plan, required several translations with the traversing mechanism to scan the complete fluid width for one projection angle. This is because the diameter of the laser beam was only 70mm. the data thus percorded in the form of images were joined together using computer programs to generate one complete image corresponding to a given projection angle.

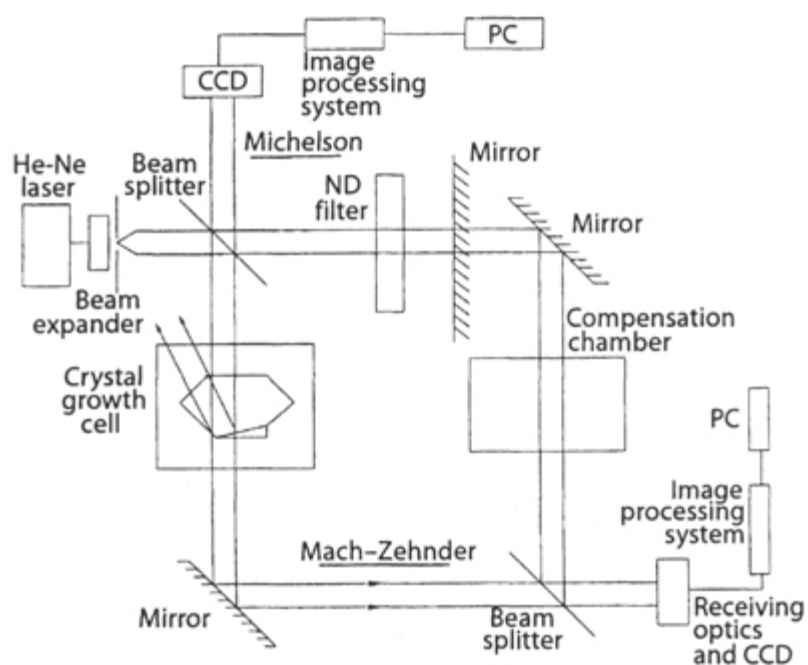


Figure 4.15: Combined Mach-Zehnder and Michelson interferometry for crystal growth from a solution

Module 4: Interferometry

Lecture 18: Applications, literature review, interferometry

The Mach-Zender interferometer can be operated in two modes, namely the (a) infinite fringe setting, and the (b) wedge fringe setting. In (a) the test and reference beams are set to have identical geometrical path lengths and fringes from due to density, and so temperature, changes alone (In this discussion, changes in density due to changes in pressure are taken to be of secondary importance; this assumption is valid for many buoyancy-driven flow experiments). Since each fringe is a line of constant phase, it is also a line of constant refractive index, a line of constant density, and, hence temperature, and hence an isotherm. It can also be shown that the fringe thickness is an inverse measure of the local temperature gradient, being small where gradients are high. The infinite fringe setting is employed for high-accuracy temperature measurements in the fluid. In (b), the mirrors and beam splitters are deliberately misaligned to produce an initial fringe pattern of straight lines. When a thermal disturbance is introduced in the path of the test beam, these lines deform and represent the temperature profiles in the fluid. The wedge fringe setting is commonly employed for wall heat flux measurements.

The specifications of the components of a Mach-Zehnder interferometer employed by the author are presented below.

Table 1: Specifications of the He-Ne Laser

Make	Spectra-Physics
Model	Spectra-Physics 127
Output Power	60 mW(maximum), 35 mW average output
Wavelength	632.8 nm
Color	Orange Red
Coherence Length	20-30 cm
Power Consumption	≈ 0.1kW of electrical power
Efficiency	0.01 – 0.1%
Beam Diameter	1.25 ± 0.10mm
Beam Divergence	0.66 ± 0.06 mrad
Amplitude Noise, 10 Hz-2MHz	< 1% rms
Amplitude Ripple, 45 Hz-1kHz	< 1% rms
Life Time	≈ 20,000 hours of operation

Module 4: Interferometry

Lecture 18: Applications, literature review, interferometry

To illustrate fringe formation in the infinite fringe setting, a candle flame was put in the path of the test beam and the Interferograms was recorded. The candle flame in the infinite fringe setting is shown in [figure 4.11](#). The fringes can be seen to correspond to isotherms around the candle flame.

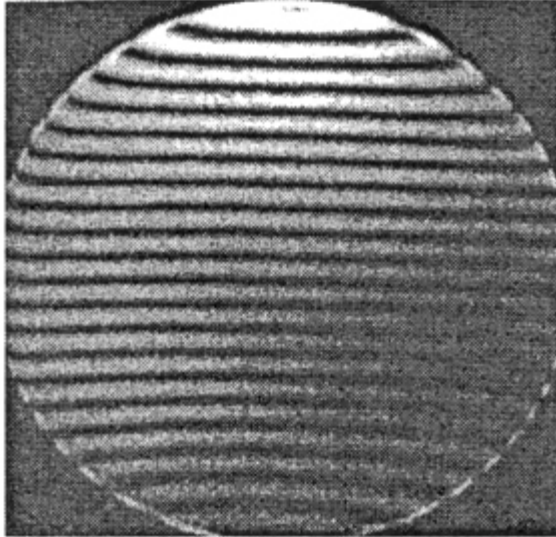


Figure 4.12: Wedge Fringe setting of the interferometer

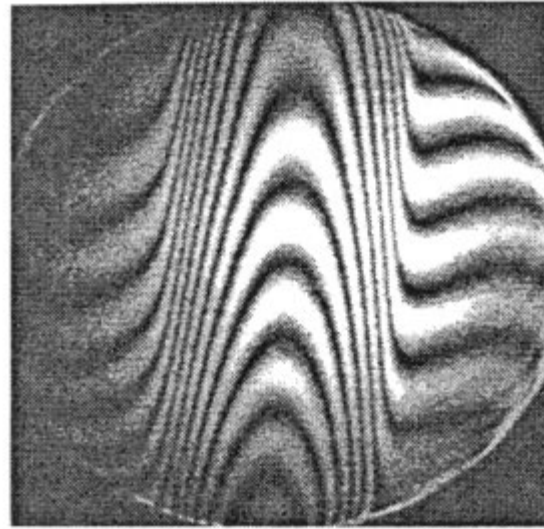


Figure 4.13: Candle Flame in the wedge fringe setting

The wedge fringe setting is comparatively easier to setup than the infinite fringe setting. Here the initial fringes are due to deliberate misalignment between the optical components. Initially the fringes are adjusted so that they are perfectly straight. Figure 4 shows the initial wedge fringe setting of the interferometer. If a thermal disturbance is introduced in the path of the test beam, the fringes get displaced to an extent depending on the nature of the temperature profile. Hence the fringes in the wedge fringe setting of the interferometer are representative of the temperature profile in the fluid medium under study. The candle flame experiment is shown in the wedge fringe setting mode in [figure 5](#). Here the fringes are the temperature profile inside the flame.

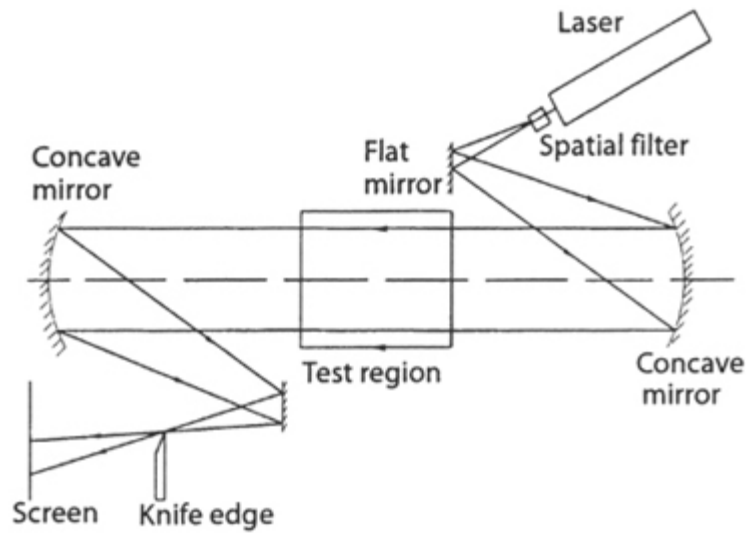


Figure 4.14 (a): Schematic drawing of a schlieren apparatus

For completeness, the schlieren and shadowgraph configurations are shown in figures 4.14 (a) and 4.14 (b), respectively. A combined Mach-Zehnder and Michel son interferometer for simultaneous measurement of thermal convection and crystal topography is shown in figure 4.15.

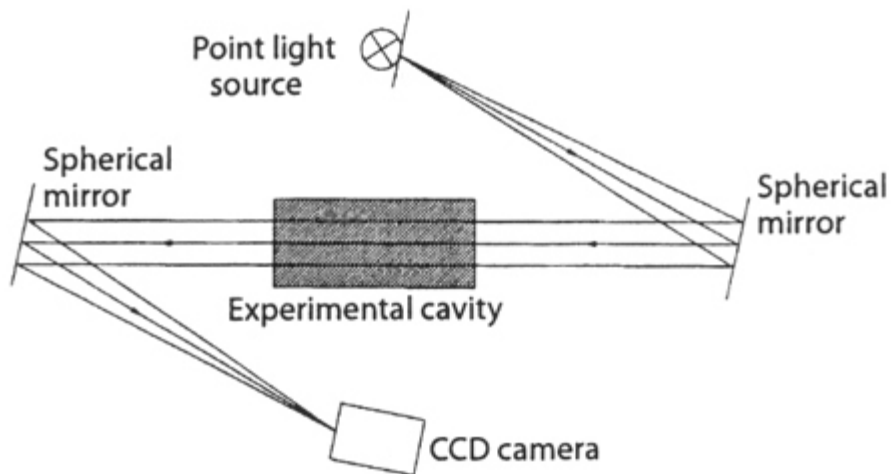


Figure 4.14 (b): Schematic drawing of a shadowgraph apparatus